

A comparison of the embryonic stem cell test and whole embryo culture assay combined with the BeWo placental passage model for predicting the embryotoxicity of azoles



Myrto Dimopoulou^{a,b,*}, Aart Verhoef^b, Caroline A. Gomes^d, Catharina W. van Dongen^{a,d},
Ivonne M.C.M. Rietjens^a, Aldert H. Piersma^{b,c}, Bennard van Ravenzwaay^{a,d}

^a Division of Toxicology, Wageningen University, The Netherlands

^b National Institute of Public Health and the Environment (RIVM), Bilthoven, The Netherlands

^c Institute for Risk Assessment Sciences (IRAS), Utrecht University, Utrecht, The Netherlands

^d BASF SE, Experimental Toxicology and Ecology, Ludwigshafen, Germany

ARTICLE INFO

Keywords:

Whole embryo culture
Stem cell test
Placental transfer
Azoles
Biomarkers
Embryotoxicity

ABSTRACT

In the present study, we show the value of combining toxico-dynamic and -kinetic *in vitro* approaches for embryotoxicity testing of azoles. Both the whole embryo culture (WEC) and the embryonic stem cells test (EST) predicted the *in vivo* potency ranking of twelve tested azoles with moderate accuracy. Combining these results with relative placental transfer rates (Papp values) as determined in the BeWo cell culture model, increased the predictability of both WEC and EST, with R^2 values increasing from 0.51 to 0.87 and from 0.35 to 0.60, respectively. The comparison of these *in vitro* systems correlated well ($R^2 = 0.67$), correctly identifying the *in vivo* strong and weak embryotoxicants. Evaluating also specific gene responses related with the retinoic acid and sterol biosynthesis pathways, which represent the toxicological and fungicidal mode of action of azoles respectively in the WEC and EST, we observed that the differential regulation of *Dhrs3* and *Msmo1* reached higher magnitudes in both systems compared to *Cyp26a1* and *Cyp51*. Establishing sensitive biomarkers across the *in vitro* systems for studying the underlying mechanism of action of chemicals, such as azoles, is valuable for comparing alternative *in vitro* models and for improving insight in the mechanism of developmental toxicity of chemicals.

1. Introduction

The risk assessment of chemicals is still highly dependent on the use of experimental animals (Augustine-Rauch et al., 2010; van der Jagt et al., 2004). Additionally, complying with the European chemical safety legislation (REACH), the number of experimental animals will dramatically increase, reaching an estimated 22 million vertebrates (Piersma, 2006; Scialli, 2008). Reproductive and developmental toxicology requires the highest percentage of experimental animals, which may reach an estimated 60% (Rovida and Hartung, 2009; Scialli and Guikema, 2012). Over the past decades, awareness has risen about the necessity of developing alternative approaches to animal testing for reducing, refining and replacing the animal testing (Adler et al., 2011). A number of *in vitro* alternative assays have been developed for screening developmental toxicants, including cell lines, single organs and whole embryo cultures. The European Centre for the Validation of Alternative Methods (EVCAM) has already validated the Embryonic

Stem Cell test (EST), the limb bud micromass test and the rat Whole Embryo Culture (WEC) assay as alternative *in vitro* tests for studying the developmental toxicity of xenobiotics (Lee et al., 2012; Piersma, 2006; Sogorb et al., 2014).

Among these alternative tests for screening developmental toxicity, only the EST does not require the use of animals or animal-derived tissue (Sogorb et al., 2014; Spielmann, 2009). Murine pluripotent embryonic stem cells can be isolated, cultured and further differentiated to a variety of cell-types, such as cardiomyocytes, neural, red blood cells and others (Genschow et al., 2004; Spielmann et al., 1997). One requirement for the differentiation is the formation of multicellular aggregates, the embryonic bodies (EBs), which allows the induction of cells of endo-, meso- and ectoderm after continuous *in vitro* culture, mimicking the egg-cylinder stage of an *in vivo* 5-day old embryo (Doetschman et al., 1985). However, the EST is a simplified method, as only one morphological endpoint, the assessment of contracting cardiomyocytes following the 10-day differentiation protocol, is

* Corresponding author at: Wageningen University, Division of Toxicology, P.O. Box 8000, 6708 WE, Wageningen, The Netherlands.
E-mail address: myrto.dimopoulou@wur.nl (M. Dimopoulou).

considered. Originally, in the validated EST method by the EVCAM, in addition to the ES-D3 differentiation and cytotoxicity assays, the effect of chemicals in the 3T3 fibroblast cells was added as an indication of maternal toxicity (Genschow et al., 2004). Although an indication of maternal toxicity could be obtained, the relevance of this information compared to the *in vivo* situation is debatable (Marx-Stoelting et al., 2009). Additionally, the EST lacks both the complexity and programmed pattern formation of a whole organism and has not any metabolic capacity (Piersma, 2006; Sogorb et al., 2014). The rat WEC is a more complex model, which mimics quite well the *in vivo* situation (Ellis-Hutchings and Carney, 2010; Webster et al., 1997). A variety of morphological endpoints, quantitatively summarized as a total morphological score, is evaluated for concluding about any possible effect on the embryonic growth and development (Brown and Fabro, 1981; New, 1978). This model covers gestational day (GD) 10–12, when neurulation and organogenesis occur. This critical time window gives an important advantage for closely monitoring the developmental toxicity in the rat WEC, but on the other hand is one of the restrictions of the system as it is not applicable for other time windows of development (Piersma, 2006; Piersma et al., 2004).

One common disadvantage of EST and WEC is the different exposure situation compared to *in vivo*, including the absence of placenta (Blaauboer, 2010). The placenta is an important organ during the pregnancy, required for the transportation of nutrients, oxygen and hormones from the mother to the fetus, as well as for removing waste products from the embryonic side (Benirschke et al., 2006; Prouillac and Lecoeur, 2010). Xenobiotics are differently transferred across the placenta according to their physicochemical properties (Pacifci and Nottoli, 1995). Therefore, the evaluation of possible effects on the placenta as well as the addition of toxicokinetic information derived from placental exposure to xenobiotics could improve the predictability of *in vitro* systems, designed for assessing developmental toxicity (Blaauboer, 2010; Myllynen et al., 2005; Strikwold et al., 2013). As described by Poulsen et al. (Poulsen et al., 2009), the *ex vivo* placental perfusion model is a human-based system for studying the transport of xenobiotics across the placenta with the highest relevance to the *in vivo* situation. However, this model is laborious and dependent on the availability of fresh placentas that are donated from mothers after deliveries (Poulsen et al., 2009). An alternative to the *ex vivo* placental perfusion model is the BeWo transport assay, which is easy, fast and cheap. The BeWo b30 cell line, human chorioncarcinoma derived cells, grow on permeable membranes from transwell inserts and form a confluent cell layer (the BeWo layer) (Bode et al., 2006; Mitra and Audus, 2008; Poulsen et al., 2009). Using the transwell system, it is possible to mimic the *in vivo* situation, by dividing the well in the basolateral and apical compartments, which are related to the maternal and embryonic sides, respectively (Li et al., 2013). By exposing the apical compartment to the xenobiotic under assessment, its transportation to the basolateral compartment can be measured. Consequently, the assessment of embryotoxic profiles of xenobiotics in the EST and the rat WEC, in combination with the BeWo model, could enable the evaluation of the morphologically evaluated effects at concentrations that have been corrected for the placental transfer (Li et al., 2016, 2015).

Furthermore, because gene expression responses precede the corresponding morphological changes and, consequently, could predict them, gene expression studies could be further implemented here for elucidating the mode of toxicological action of the testing compounds (Daston and Naciff, 2010; Robinson et al., 2012a; Robinson and Piersma, 2013; Romero et al., 2015). Consequently, the combination of more *in vitro* assays with multi-target readouts may improve the predictions of embryotoxic responses, distinguishing classes of chemicals or identifying unique signatures within the same chemical group (Adeleye et al., 2015; Estevan et al., 2014; Krewski et al., 2010; Piersma et al., 2013).

Azoles are antifungal agents with agricultural and clinical use (Marotta and Tiboni, 2010). They have been designed to interact with

the sterol biosynthesis pathway and further inhibit the fungal *Cyp51*, which is the catalyst for converting lanosterol to ergosterol, disturbing the fungal cell-membrane integrity (Georgopapadakou, 1998; Marotta and Tiboni, 2010). Some of the azoles have previously shown embryotoxicity in *in vivo* systems, mainly introducing abnormalities related with craniofacial alterations and skeletal dysmorphogenesis (de Jong et al., 2011; Dimopoulou et al., 2017a; Hermsen et al., 2012; Li et al., 2015; Robinson et al., 2012c; van Dartel et al., 2011). The main cause of their observed embryotoxicity has been postulated to be their interaction with retinoic acid (RA)-related enzymes, such as *Cyp26a1* and *Dhrs3*, which are modulators of the RA homeostasis in mammalian systems by regulating the metabolism or synthesis of RA, respectively (Dimopoulou et al., 2016; Luijten et al., 2010; Piersma et al., 2017; Robinson et al., 2012c). RA has been shown to be a morphogen in vertebrate embryogenesis (Piersma et al., 2017; Tonk et al., 2015).

In the present study, twelve azoles were tested in the EST and the obtained results were compared to WEC assay results, which have been reported in our previous study (Dimopoulou et al., 2017b). Furthermore, their placental transport rates, obtained with the BeWo model, were combined with the effective concentrations in the EST and WEC, to assess if an improvement of the correlation between *in vitro* and *in vivo* developmental toxicity (potency ranking) could be achieved. We also compared the expression of four genes, two biomarkers of the toxicological (*Cyp26a1* and *Dhrs3*) and two of the intended fungicidal (*Cyp51* and *Msmo1*) mode of action of azoles. The selection of these genes as potential gene-biomarkers of the pathways of interest was based on the results of our previous study on the transcriptome of rat WEC exposed to the same compounds (Dimopoulou et al., 2017b), as well as on literature data with which Robinson et al. showed the increased regulation of these genes in both systems, including also the zebrafish embryo test (ZET), when exposed to azole compounds (Robinson et al., 2012b).

2. Materials and methods

2.1. Chemicals

Nine azoles compounds were purchased from Sigma-Aldrich (Zwijndrecht, The Netherlands); flusilazole (FLU; CAS# 85509-19-9); difenoconazole (DFZ; CAS# 119446-68-3); ketoconazole (KTZ; CAS# 65277-42-1); prothioconazole (PTZ; CAS# 178928-70-6); triadimefon (TDF; CAS# 43121-43-3); fenarimol (FEN; CAS#60168-88-9); propiconazole (PRO; CAS#60207-90-1); and tebuconazole (TEB; CAS#107534-96-3). Miconazole (MCZ, CAS# 22916-47-8) was purchased from Sigma-Aldrich and Alfa Aesar (Germany). BASF SE (Ludwigshafen, Germany) kindly provided three novel azoles, encoded as B595, B599 and B600, of which the chemical structures are shown in Fig. 1. All the compounds, tested in the EST, were dissolved in dimethyl sulfoxide (DMSO, Sigma-Aldrich, Zwijndrecht, The Netherlands) at 0.25% v/v final concentration in the culture medium. Antipyrine (CAS# 60-80-0) and amoxicillin (CAS# 26787-78-0) were purchased from Sigma (Germany) and were used as controls for high and low permeability in the BeWo transport tests, respectively. They were dissolved in DMSO at a maximum 0.5% v/v final concentration in HBSS (Biochrom, Germany) in cell culture. Fluorescein (CAS# 2321-07-5, Sigma, Germany) was used as paracellular transfer control in the BeWo model and was dissolved in HBSS at a final concentration of 20 μ M.

2.2. Embryonic stem cell test (EST)

2.2.1. Pluripotent stem cell culture

Murine D3 embryonic stem (ES-D3) cells (ATCC, Rockville, MD) were cultured in polystyrene cell culture petri dishes of 35 mm diameter (Corning) in humidified atmosphere at 37 °C and 5% CO₂ and they were routinely subcultured every 2–3 days. They were maintained in culture medium, which consisted of Dulbecco's modified Eagle's medium

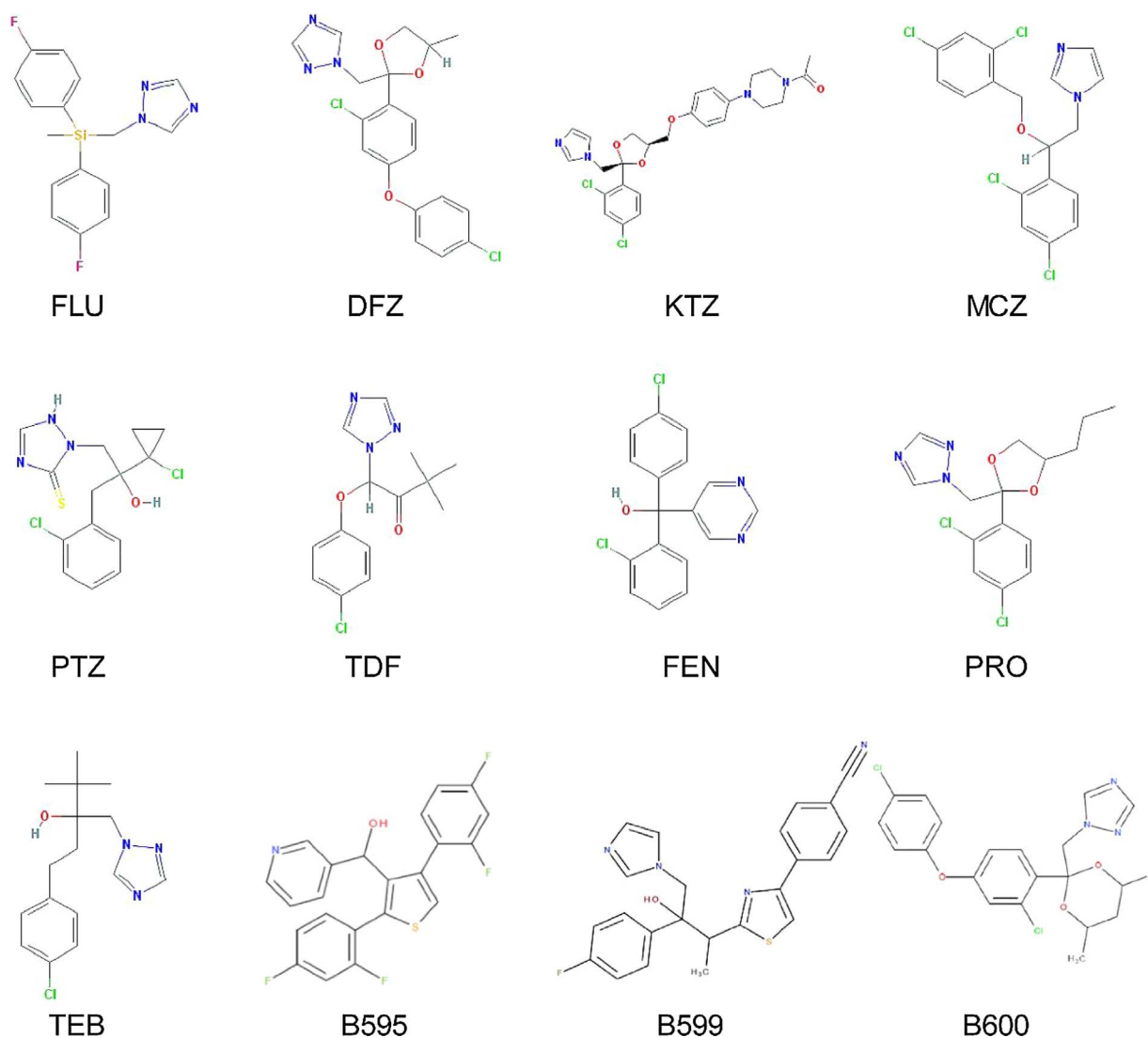


Fig. 1. Chemical structures of the twelve azoles under assessment.

(DMEM, Gibco) supplemented with 20% fetal bovine serum (Greiner Bio-One), 1% non-essential amino acids (Gibco), 1% penicillin/streptomycin (Gibco), 2 mM L-glutamine (Gibco) and 0.1 mM β -mercaptoethanol (Sigma-Aldrich). To maintain the pluripotency of the ES-D3 cells, murine leukemia inhibitor factor (mLIF; ESGRO, Millipore, the Netherlands) was directly added to the culture petri dish at a final concentration of 1000 units/mL.

2.2.2. Cardiomyocyte differentiation assay

Cardiac differentiation of ES-D3 cells was performed according to the protocol (Genschow et al., 2004) using the previously described culture medium without containing mLIF. In brief, stem cell suspensions of 15×10^4 cells/mL were further diluted to 3.75×10^4 cells/mL and placed on ice before starting the hanging drops protocol. Next, 20 μ L of stem cell suspension was placed on the inner part of the lid of a 100 mm diameter petri dish (Greiner Bio-One) containing 5 mL phosphate buffered saline (PBS, Gibco), Ca^{2+} and Mg^{2+} free, resulting to hanging drops. Each petri dish contained 56 drops, and each drop consisted of 750 cells. The dishes were cultured for three days at 37 °C and 5% CO_2 , during which the ES-D3 proliferated and formed cell-aggregates, called embryonic bodies (EBs). On day three, EBs were transferred to a 60mm-diameter bacterial petri dish (Greiner Bio-One), containing 5 mL culture medium without mLIF, and were further cultured under the same conditions for two days. After, each individual EB

was transferred to a single well in a 24-well plate (TPP, Trasadingen, Switzerland), containing 1 mL culture medium without mLIF. After five days, the cardiac differentiation was microscopically determined by examining whether the EBs had turned into contracting myocardial cells. The plates were scored as positive or negative based on the presence or absence of contracting myocardial cells, respectively. For each test compound, the chemical exposure started at the differentiation day 3 and refreshed at day 5 when EBs were transferred in a new plate-setup. Except for KTZ, all the tested compounds were tested at a range of concentration from 0.01 μ M to 300 μ M. The highest concentration at which KTZ tested was 100 μ M. For each compound, three independent experiments were performed (biological replicates), while each experimental day the experiments were performed in duplicates (technical replicates). Additionally, solvent and medium control cultures were separately observed for each of the tested compounds. Tests were accepted when 21 out of 24 EBs exposed to the solvent control (0.25% v/v DMSO) were contracting. The number of positive EBs was expressed as fraction of total control (24 EBs).

2.2.3. Cell viability assay

ES-D3 cells were seeded in a 96-well plate (Greiner Bio-One) diluted to 1×10^4 cells/mL (500 cells per well) in culture medium containing mLIF and incubated at 37 °C and 5% CO_2 to allow cell adherence. Afterwards, 150 μ L culture medium was added to full-fill each well up

to 200 μ L volume. After continuous incubation for three days, the culture medium was removed and replaced with freshly made exposure medium (200 μ L), supplemented with mLIF and containing the corresponding test compound and concentration for each exposure. On day 5, 100 μ L of the supernatant medium was removed and 20 μ L of CellTiter-Blue (G8081, Promega, Leiden, the Netherlands) was added in each of the wells and incubated for two more hours. The assay measures the metabolic capacity of viable cells exposed to the tested chemicals to reduce resazurin (blue) into resorufin (pink), which is highly fluorescent. The non-viable cells lose this metabolic capacity and, therefore, they do not generate a fluorescent signal. The fluorescence was read using SpectraMax[®] M2 spectrofluorometer (Molecular Devices, Berkshire, United Kingdom) at 544 nm and 590 nm (excitation and emission, respectively). Two independent experiments, in six technical replicates each, were performed for each of the tested compounds. Solvent (0.25% v/v DMSO), positive (0.1 μ g/mL 5-FU) and negative (500 μ g/mL Penicillin) controls were included in every experiment in six replicates.

2.2.4. Concentration-response curves and determination of both ID_{50} and IC_{50}

Results from the EST were analysed and concentration-response curves were fitted using the PROAST software (Slob, 2002). Based on the fit of the curve and with 95% confidence intervals, we calculated the concentration (ID_{50}) at which the number of contracting cells were reduced to 50% of the control (0.25% v/v DMSO). Following the same rationale, we also calculated the IC_{50} concentration at which exposed cells resulted to 50% decrease in cell viability by analysing the data obtained from the corresponding assays. The calculated ID_{50} concentration for each of the tested compounds was further applied for performing the gene expression studies.

2.2.5. EST exposure to azoles for gene expression analysis

Following the cardiomyocyte differentiation protocol, we exposed the EBs on day 3 at the ID_{50} of each of the tested azoles, as calculated from the cardiomyocyte differentiation assay, and we collected them after 24 h of exposure (day 4) in eppendorf tubes, containing 800 μ L RNAprotect (Qiagen, Cat. # 76526), which were further stored at -20°C prior to RNA extraction. Concurrent solvent (0.25% v/v DMSO) and culture medium controls were collected similarly to the exposed cultures. All the exposure groups consisted of 8 replicates and the control groups contained 12 replicates. Additionally, extra plates containing EBs (three independent experiments in duplicates) exposed to the tested azoles at their ID_{50} were further cultured, following the 10-day EST differentiation protocol. Then, they were microscopically examined to determine whether the efficiency of the applied concentration for inhibiting the cardiomyocyte contraction is indeed 50%. Three independent experiments, in technical duplicate each, were performed, including also solvent and culture medium controls.

2.2.6. RNA isolation

Before starting the RNA isolation, samples were thawed on ice. RNA was further isolated using the RNeasy Mini-extraction kit (Qiagen, Cat. # 74104), following manufacturer's protocol. In brief, tubes containing the EBs were spun down and excess volume of RNAprotect was discarded. Then, we added the RLT buffer and by gently pipetting the EBs were broken down into smaller pieces. We treated the samples with QIAshredder (Qiagen, Cat. # 79654) for better homogenization and therefore, for increasing the RNA yields. Then, the lysates were transferred into RNeasy spin columns for purifying the RNA extracts. We additionally treated the extracts with the RNase-Free DNase set (Qiagen, Cat. # 79254), for achieving better purification. Quantity and quality of RNA yields were determined with Nanodrop (Nanodrop Technologies Inc., Wilmington, Delaware) and 2100 BioAnalyzer (Aligent Technologies, Amstelveen, the Netherlands). Samples with absorbance values between 1.9 and 2.2 (ratio 260 nm/280 nm) and

RNA integrity number (Spielmann et al.) higher than 8 were further used for performing the gene expression study.

2.2.7. Gene expression with Real-Time PCR

For performing the RT-PCR analysis, cDNA was synthesized by using the high-capacity cDNA archive kit containing random hexamer primers (Applied Biosystems, Foster City, CA, Cat. # 4368814), according to manufacturer's instructions. The quantification of the mRNA of the genes of interest was measured with TagMan gene expression assays (Applied Biosystems) on a 7500 Fast Real-Time PCR system. We followed the two-step PCR protocol provided by the manufacturer, which included the following thermal cycling conditions: 95°C for 20 s for the first cycle, followed by 40 cycles of 95°C for 3 s and 60°C for 30 s. The measured mRNA markers were *Cyp26a1* (Applied Biosystems, Cat. # Mm00514486_m1), *Dhrs3* (Applied Biosystems, Cat. # Mm00488080_m1), *Cyp51* (Applied Biosystems, Cat. # Mm00490968_m1) and *Msmo1* (Applied Biosystems, Cat. # Mm00499390_m1). The used housekeeping genes were *Hprt1* (Applied Biosystems, Cat. # Mm03024075_m1) for *Cyp26a1* and *Dhrs3*, and *Polr2a* (Applied Biosystems, Cat. # Mm00839502_m1) for *Cyp51* and *Msmo1*. The No Template Control (NTC) and No Reverse Transcriptase (no RT) control were included in every RT-PCR run for assessing the reliability of the produced results. The mRNA expression was normalized to the value of *Hprt1* or *Polr2a* for each of the reactions according to the comparative Ct method ($\Delta\Delta\text{Ct}$) and the obtained results were relatively expressed in fold induction of gene expression.

2.2.8. Gene expression analysis-data processing

The parametric Student's *t*-test two-sided with $p < 0.05$ approach was used for determining the statistical significance on the expression of the selected genes in EST exposed to chemicals compared to this exposed to the solvent control (DMSO). All the exposure and control (DMSO and medium) groups consisted of 8 and 12 samples, respectively.

2.3. BeWo transport model

2.3.1. BeWo b30 culture

The BeWo b30 culture and transport experiments were performed as described in Li et al. (Li et al., 2016; Li et al., 2015) with slight adaptations. The BeWo b30 cell line was purchased from AddexBio (Cat. # C0030002, Lot. # 7985832; San Diego, USA). It was confirmed to be bacteria, yeast and mycoplasma negative (certificate of analysis from AddexBio). For maintaining and culturing the BeWo cell line, Dulbecco's Modified Eagle's Medium (DMEM) (Cat. # FG0445), HBSS without phenol red with $\text{Ca}^{2+}\text{Mg}^{2+}$ (Cat. # L2035), Fetal Bovine Serum (FBS) Superior (Cat. # S0615, Lot. # 0114F), Penicillin/Streptomycin solution (Cat. # A2213), Trypsin/EDTA 0.05%/0.002% (Cat. # L2143) and PBS without $\text{Ca}^{2+}\text{Mg}^{2+}$ (Cat. # L1825) were purchased from Biochrom, Germany. Sodium Pyruvate (Cat. # 11360-039) was purchased from Gibco Life Sciences, Germany. BeWo b30 cells (passages 24–36) were routinely subcultured, 3 to 4 times per week, and maintained in polystyrene cell-culture flasks (TRP, Switzerland) in culture medium consisted of DMEM supplemented with 10% (v/v) FBS, 1% (v/v) Penicillin/Streptomycin solution and 1% (v/v) Sodium Pyruvate under a humidified atmosphere of 5% CO_2 at 37°C . The cells were harvested after their treatment with 0.05% trypsin-EDTA solution. For their subculture (passage), they were seeded in a new cell culture flask at a density of 2 to 2.5×10^6 cells/flask and incubated at 37°C and 5% CO_2 . For transport experiment, they were transferred to 12-well plates with transwell polycarbonate membranes (12 mm diameter, 0.4 μm pore size; Cat. # 3401, Corning Costar, USA) pre-coated with human placental collagen type IV (Cat. #5533, Sigma-Aldrich), where they were seeded at a density of 1×10^5 cell/ cm^2 in a 0.5 mL volume (apical compartment), while the basolateral compartment contained 1.5 mL culture medium. The culture conditions were the same as during the

simple cell maintenance (37 °C and 5% CO₂). The medium in both compartments was daily changed until day 6 of post-seeding, when the transfer experiments were performed.

2.3.2. BeWo transport experiments

For the Bewo transport model, literature data obtained from Li et al. (Li et al., 2016; Li et al., 2015) and additional experimental data generated by BASF SE (Germany) were used in this study. The BeWo experimental data were generated following the methodology described in these literature studies with slight adaptations. Before starting the transfer experiments, the wells were equilibrated in HBSS in both compartments for 30 min in the incubator and transepithelial electrical resistance (TEER) values were measured using a voltmeter (EVOM X, Cat. No. 72564, World Precision Instruments, USA) with an EVOM electrode set (STx2, World Precision Instruments, USA). The plates were placed under a hot plate at 37 °C to minimize temperature effects. TEER values were corrected for collagen-coated wells without the presence of cells, and transformed in $\Omega \times \text{cm}^2$, by multiplying the measured values in Ω per the insert area (1.12 cm²). Only wells showing a TEER value $\geq 44 \Omega \times \text{cm}^2$ were used for transfer experiments. Fresh stock solutions of the compounds were made (10 mM FLU, DFZ, MCZ, TDF, amoxicillin and antipyrine in DMSO; 1 mM fluorescein in HBSS) and working solutions were made by diluting in HBSS 200 × for FLU, DFZ, TDF, amoxicillin and antipyrine, and a dilution of 1000 × for MCZ. The resulting exposure concentrations were 50 μM for FLU, DFZ, TDF, amoxicillin and antipyrine, and 10 μM for MCZ, with a maximum concentration of 0.5% DMSO in any case. These chosen concentrations were based on the preparatory cell viability experiment results, which showed that the cell viability of 3-day BeWo cells was not affected after exposure to 50 μM of FLU, DFZ and TDF. However, due to decreased cell viability at the concentration of 20 μM of MCZ (75.9 \pm 3.0% viability), the BeWo transport experiments for MCZ were performed at 10 μM . Fluorescein was diluted 50 times in HBSS leading to an exposure solution of 20 μM , which was added at the performed experiments as a paracellular control (restricted transfer in the presence of BeWo cells). During the substance preparation and transfer experiments, the test compounds were protected from light exposure due to their increased sensitivity (especially for MCZ and fluorescein). Starting the transport experiments, 0.5 mL of the exposure solutions of each of the test substances and controls were added into the apical compartment and 1.5 mL of HBSS (transport buffer) to the basolateral compartment. Directly after exposure, 0.2 mL samples of the exposure solutions (in triplicate) were collected in 96 deep well plates (Thermo Fisher Scientific, Germany). After 15, 30, 60 and 90 min of plate incubation in a humidified atmosphere with 5% CO₂ at 37 °C, samples of 0.2 mL were collected from the basolateral compartment and replaced by an equal volume of HBSS. At the end of the transport experiments, an additional sample of 0.2 mL was collected from the apical compartment, for calculating the recovered amount of every tested compound. In each transport experiment, antipyrine and amoxicillin were included as controls of high and low permeability of the BeWo layers, respectively. Collected samples were stored at –20 °C for further determining their transport rates by LC–MS analysis, conducted at the contract research organization Pharmacelsus GmbH (Germany).

In the end of the transport experiments, the transwells were washed twice with HBSS and equilibrated for 30 min in the incubator, with 0.5 mL HBSS in the apical, and 1.5 mL HBSS in the basolateral compartment. TEER was measured again using the previously described method. Hereafter, 0.5 mL of MTT working solution and 1.5 mL of culture medium were added to the apical and basolateral compartments, respectively. After incubation of 30 min at 37 °C, MTT (apical compartment) was replaced by 800 μL 95% DMSO in HBSS. After 30 s of shaking, 150 μL of samples from the apical compartment were collected and divided in triplicate in a 96-well plate (TRP, Switzerland). The absorbance was measured at wavelengths 570 and 690 nm using spectrophotometer (Wallac Equipment).

2.3.3. Ultra-high performance liquid chromatography (UHPLC) analysis

Samples were analysed using the Accela 1250 ultra-high performance liquid chromatography (UHPLC) to quantify the amount of the tested azoles that were transferred from the apical to basolateral compartment and, based on these data, to calculate their transport rates and relative Papp values. Samples with 3 μL injection volume were separated on an analytical column (Accucore PFP, 2.6 μm , 50 cm \times 2.1 mm) with a pre-column (C6-Phenyl, 4 cm \times 2 mm, Phenomenex, Germany). The UHPLC was performed in the gradient mode using acetonitrile + 0.2% heptafluoro butyric acid (HFBA), as the organic phase, and 0.1% formic acid (FA) in nanopure water, as aqueous phase. Eluents were pumped (Dionex UltiMate 3000 RS pump) with a flow rate of 0.6 mL/min. Measurements applying the Orbitrap™ technology with the Q-Exactive plus mass spectrometer (MS) were used to analyze the samples. As MS tune file, a generic tune file was used. The $[\text{M} + \text{H}]^+$ ion of the diisooctyl phthalate (m/z 391.28429), which is ubiquitously present in the solvent system, was used as a lock mass for internal mass calibration. The MS was operated in the positive full scan mode, the accurate masses of the monitoring ions \pm 5 mDa were used for test item and internal standard peak integration. Further analyzer settings were as follows: maximum injection time 150 ms, sheath gas 40, aux gas 10, sweep gas 2, spray voltage 3.8 kV, capillary temperature 350 °C and heater 350 °C. For analyzing the LC–MS data, the operating software Xcalibur 4.0.27.19 was used.

2.3.4. Analysis of BeWo transport data

For each of the test compounds, the concentration of the samples collected at 0, 15, 30, 60 and 90 min from the basolateral, as well as from a sample from the apical compartment at 90 min were determined and converted to nmol. For each compound, the linear appearance rate in the basolateral compartment was calculated, used for estimating the apparent permeability (Papp) coefficients, according to the following formula:

$$\text{Papp coefficient} \left(\frac{\text{cm}}{\text{s}} \right) = \frac{\frac{\Delta Q}{\Delta t}}{A \times C_0}$$

For calculating the amount of the test compound ΔQ (nmol), transported to the basolateral chamber after certain duration of the transport experiment, Δt (s), we applied the following formula: ΔQ at t_{x+1} = [amount determined at t_{x+1} (μM) \times 1.5 mL] + [amount removed at t_x (μM) \times 0.2 mL]. A (1.12 cm²) is the insert surface area and C_0 is the determined actual exposure concentration (μM) in the beginning of the transport experiment ($t = 0$). The relative Papp values were calculated by dividing the Papp coefficient values of each test compound with the Papp coefficient value of antipyrine (reference compound). The recovery of each test compounds was also calculated by adding the amount (nmol) of the compound in the apical and basolateral compartment at t_{90} , adjusted with the actual exposure amount (nmol) in the apical compartment (0.5 mL), which was set at 100%.

2.4. In vivo data analysis

As previously described, we collected literature data regarding the *in vivo* developmental toxic profile of the twelve tested azoles (Dimopoulou et al., 2017b). In brief, we selected studies performed in rats, which were orally exposed to the tested compounds during either GD 6–15 or GD 7–16 at multiple dose regimes. Studies with at least one control group and two dose groups were selected to allow analysis using the Benchmark Dose (BMD) approach. The BMD values were calculated based on the evidence of sensitive endpoints of *in vivo* developmental toxicity. A concentration-response curve was fitted to the data to determine the BMD for the selected benchmark response (BMR) for each tested azole. The BMD was defined as 10% additional incidence of developmental toxicity (BMD₁₀) with the US EPA BMD software. Among the several models that were fitted, the selection of the best

model was determined based on the goodness of fit (p -value > 0.05). The *in vivo* prenatal developmental toxicity data for the three new azoles were provided by BASF. For the three novel compounds, given the available data, we proceeded with a qualitative *in vivo* potency ranking concept, which was adjusted and applied in our study, including also the nine commercially available compounds. For implementing this approach of *in vivo* analysis, the profiles of the tested compounds were characterized as potent, moderate and weak or non-potent.

2.5. Correlation tests

To determine the relationship between the different alternative assays (EST and WEC), with or without their combination with the BeWo transfer model, we plotted their calculated ID₅₀ against ID₁₀ values, respectively. The ID₁₀ concentrations in the rat WEC were obtained from our previous study (Dimopoulou et al., 2017b). Then, we fitted a line based on minimizing the sum of residuals of the horizontal and vertical distances of the data to the line, to which fit is characterized by the coefficient of determination R², representing the fraction of variation. For evaluating whether any of the alternative *in vitro* assays could better predict the *in vivo* developmental toxic profile of the tested azoles, we plotted the *in vivo* BMD₁₀ concentrations versus the calculated ID₅₀ or ID₁₀ in the case of the EST or WEC, respectively. Additionally, we corrected the calculated ID₅₀ and ID₁₀ values with the relative Papp values to evaluate whether their correlations with the *in vivo* BMD₁₀ values may be improved.

Moreover, we investigated how the expression of the four genes of interest correlates in the two *in vitro* systems, WEC and EST, which could be further associated with the induced developmental toxic profile in rat embryos due to exposure to the tested azoles. The expression of the selected genes were obtained from our previous transcriptomics analysis (Dimopoulou et al., 2017b).

3. Results

3.1. Effect of azoles in inhibiting the differentiation of ES-D3 cells

All azoles induced a concentration-dependent inhibition of cardiomyocyte differentiation in the EST (Fig. 2). Except for MCZ and B595, all the ID₅₀ values were observed at concentrations much lower than those that caused cytotoxic effects on the cells, assuring that the effects did not occur due to cytotoxicity, but because of differentiation inhibition by the test compound. B599, KTZ and DFZ were the most potent azoles, showing ID₅₀ values in a range of 7–14 μM. ID₅₀s of MCZ, FLU, TDF, B600 and B595 were between 20 and 37 μM. TEB, FEN and PRO were moderately strong embryotoxicants in the EST, revealing ID₅₀s ranging between 55 and 80 μM. PTZ was the weakest azole with an ID₅₀ at 122 μM.

3.2. In vitro transport of compounds in the BeWo model

Table 1 shows the relative Papp values of twelve azoles as well as antipyrine (high permeability control) and amoxicillin (low permeability control) as used in the present study.

Before starting the transport experiments and at the end of them, the TEER values were measured for controlling the membrane integrity, showing no statistically significant change in the average of two biologically independent experiments (each performed in triplicate). Additionally, the parallel transport experiment, performed for confirming the restriction of fluorescein transport (paracellular control), was considered as an extra parameter for reassuring the validity of the obtained results (data not shown).

The transport experiments were initiated by adding in the apical compartment 50 μM for FLU, DFZ, TDF and both controls, and 10 μM for MCZ due to its cytotoxicity at 20 and 50 μM (pilot experiment, data

not shown).

Fig. 3 illustrates the amount of tested compounds detected in the basolateral compartment at different sampling times in the transport experiment. The high transwell passage of antipyrine (positive control), and the limited transport of amoxicillin (negative control), showed the validity of the performed experiments. Up to 60 min, the concentration of the azoles to the basolateral compartment increased in a linear fashion with time and, therefore, the data obtained after 60 min of incubation were used for calculating the Papp coefficient and relative Papp values (Table 1).

MCZ did not show linear transfer to the basolateral compartment through the BeWo layer, which might be related to problems with the chemical analysis, so that hardly any transport to the basolateral compartment through the BeWo layer was detected (Fig. 3), leading to unreliable Papp coefficient and relative Papp values (Table 1). We decided to exclude MCZ for further comparative analyses.

3.3. Correlations of *in vivo* and *in vitro* developmental toxicity of azoles

The BMD₁₀ value of each compound was calculated from *in vivo* prenatal developmental toxicity studies performed with each of the nine azoles (Table 2), considering abnormalities in skeleton, cleft palate formation, absence of renal papilla and hydronephrosis. For the three coded compounds provided by BASF SE, we concluded upon a qualitative potency ranking, due to limitations on the available *in vivo* data, characterizing B599, B600 and B595 as a potent, moderate and weak azole, respectively.

For assessing whether the developmental toxicity data derived from the rat WEC and EST combined with the data obtained from the BeWo placental transfer model could better predict the *in vivo* developmental toxicity, we corrected their ID₁₀ (WEC) (Dimopoulou et al., 2017b) and ID₅₀ concentrations (EST) by dividing them with their respective relative Papp values.

Based on the coefficient of correlation, Fig. 4 shows the moderately strong correlations between the ID concentrations of eleven azoles (excluding MCZ) in WEC versus EST, with close to identical R² values of 0.67 and 0.66. Figs. 5 and 6 illustrate the correlations of the *in vivo* BMD₁₀ values and the calculated ID₁₀ or ID₅₀ of nine azoles tested in the WEC and EST *in vitro* systems, respectively. We observed that the potency rankings were changed showing that in both *in vitro* models B599, KTZ and FLU were the most potent, while B600, PTZ and B595 were the weakest azoles.

For correlating the *in vivo* BMD₁₀ concentrations with the obtained *in vitro* WEC and EST ID values, we proceeded with eight compounds (MCZ was excluded as well as the three coded compounds, for which limited *in vivo* dose-response information was available). For these eight azoles, their *in vivo* BMD₁₀ concentrations were better correlated with the ID₁₀ concentrations in the rat WEC when they were corrected with the BeWo relative Papp values (R² = 0.87) compared to the non-corrected values (R² = 0.51) (Fig. 5). Similarly in Fig. 6, the corrected ID₅₀ concentrations of the eight azoles tested in the EST were better correlated with the *in vivo* BMD₁₀, resulting in an R² = 0.60, compared to the poorer correlation coefficient of 0.35 that the non-corrected ID₅₀ showed.

3.4. Quantitative comparison of gene expression changes in the EST

In a previous study in WEC (Dimopoulou et al., 2017b), we showed that early embryotoxic responses to azoles were associated with the regulation of RA-regulating genes; *Cyp26a1* and *Dhrs3*. Furthermore, in the same study, we observed that the sterol-mediated biosynthesis pathway genes, *Cyp51* and *Msmo1*, showed a more extensive response to these azoles. Now, for comparison, we quantified the expression of the aforementioned four genes in the EST, exposed to the same azoles. As illustrated in Fig. 7, the expression of *Cyp26a1* in EST exposed to any of the tested compounds at their ID₅₀s tended to be suppressed, while the

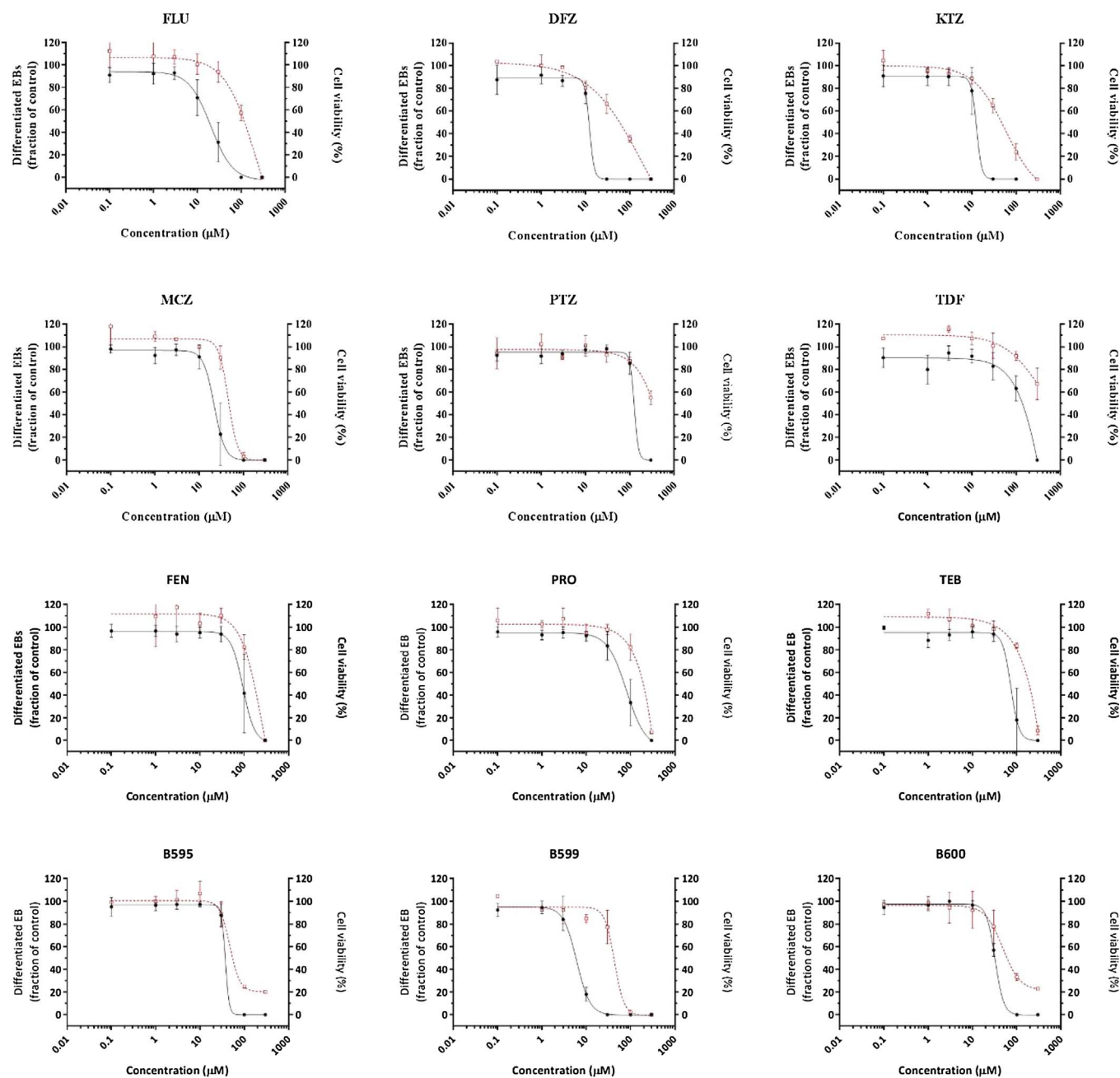


Fig. 2. Concentration-dependent effects of the twelve azoles in the EST, illustrated with the black circles (●) and black line, representing the average of three independent experiments in technical duplicates. Concentration-dependent effects of the twelve azoles on viability of the ES-D3 cells, illustrated with the red open squares (□) and red dashed line, representing the average of two independent experiments in six technical replicates. (For interpretation of the references to colour in this figure legend, the reader is referred to the web version of this article.)

expression *Dhrs3* generally showed upregulation, which was significant after exposure to FLU, MCZ and B599 with a 4.3, 3.2 and 3.3 fold change, respectively. The fold change induction of *Cyp51* in the EST ranged from 1.5 to 2.5. Additionally, the expression of *Msmo1* showed similar changes as *Cyp51*, with exposures to FLU, MCZ, TEB and PRO, reaching fold changes of 2.4, 2.6, 3.0 and 2.5, respectively. Lower fold induction of both *Cyp51* and *Msmo1* expression was observed after exposure to the ID₅₀ of PTZ, TDF and B595. Except for exposure to FEN and TEB, the upregulation of the RA related gene *Dhrs3* was higher compared to the sterol related genes, *Cyp51* and *Msmo1*.

4. Discussion

In the present study, we assessed the concentration-dependent

embryotoxicity of twelve azoles in the murine EST, by testing the inhibition of contracting cardiomyocyte differentiation (Fig. 2). We performed a cross-model comparison, using results from our previous study (Dimopoulou et al., 2017b), in which the same azoles were tested in the rat WEC. The potencies of the twelve azoles tested in the rat WEC versus the murine EST, based on the calculated ID₁₀ and ID₅₀ concentrations respectively, were reasonably well correlated ($R^2 = 0.67$). This was in agreement with the correlation that de Jong et al. have previously built using six azoles, among which two were in common with those in our study, similarly tested in the WEC and EST (de Jong et al., 2011). Both these *in vitro* models correctly detected the *in vivo* strong embryotoxicants, B599, FLU, KTZ and MCZ, as well as the weakest azoles PRO and PTZ. Considering the *in vivo* potencies of the tested azoles, their correlations with the potency ranking in the WEC and EST assays led to

Table 1

Papp coefficient and relative Papp values of twelve azoles (mean \pm SD) and the permeability controls in the BeWo model. Four of the tested azoles (including the controls) were tested in the laboratories of BASF (this paper) and the other eight were obtained from Li et al. (Li et al., 2016; Li et al., 2015), as indicated.

compound	Papp coefficient (10^{-6} cm/s) ^a	Relative Papp value
FLU ^b	24.25 \pm 3.3	0.53
DFZ ^b	9.46 \pm 2.1	0.21
KTZ ^c	31 \pm 2.4	0.79
MCZ ^b	0.87 \pm 0.7	0.02
PTZ ^c	16 \pm 2.7	0.40
TDF ^b	36.28 \pm 8.1	0.79
FEN ^c	21 \pm 3.2	0.55
PRO ^c	27 \pm 3.8	0.70
TEB ^c	33 \pm 4.3	0.86
B595 ^d	3.0 \pm 0.4	0.08
B599 ^d	18.4 \pm 1.1	0.47
B600 ^d	7.9 \pm 1.0	0.20
Amoxicillin ^b	6.75 \pm 1.1	0.15
Antipyrine ^b	46.00 \pm 3.9	1.00

^a Mean \pm SD.

^b Experimental data from this paper.

^c Obtained from Li et al. (Li et al., 2015).

^d Obtained from Li et al. (Li et al., 2016).

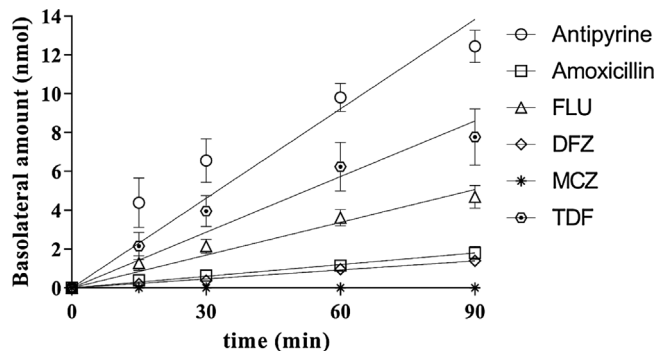


Fig. 3. The transferred amount into the basolateral compartment over time for the four tested azoles in the BeWo model, in addition to the high (antipyrine) and low (amoxicillin) permeability controls. The initial concentration was 50 μ M (25 nmol) for all the tested compounds including the controls, except for MCZ, which was tested at 10 μ M (5 nmol). Data represent the mean \pm SD of two biological replicates, each of which was performed in technical triplicate.

moderate and rather weak relationships, represented with an $R^2 = 0.51$ and $R^2 = 0.35$, respectively. The better association of *in vivo* data with those derived from the WEC model may reflect the biological complexity of WEC compared to EST (Piersma, 2006; Sogorb et al., 2014). The rat WEC contains intact embryos, which may respond to both

Table 2

Overview of *in vivo* developmental toxicity data of the nine commercially available azoles, as well as the average (\pm SD) of the calculated ID₅₀ and IC₅₀ concentrations obtained from the EST exposed to all the tested azoles, as illustrated in Fig. 1.

Compound	<i>In vivo</i> data		<i>In vitro</i> data in EST	
	<i>In vivo</i> BMD ₁₀ (μ mol/kg bw)	<i>In vivo</i> potency group	ID ₅₀ in EST average \pm SD (μ M)	IC ₅₀ in EST average \pm SD (μ M)
FLU	9.1 (Lamontia et al., 1984)	Potent	23.45 \pm 7.47	88.6 \pm 20.72
DFZ	596.5 (Lochry, 1987)	Weak	13.65 \pm 3.81	27.8 \pm 10.37
KTZ	20.1 (Tachibana et al., 1987)	Potent	13.55 \pm 11.67	18.9 \pm 6.41
MCZ	258.3 (Ito et al., 1976)	Moderate	20.5 \pm 6.38	30.6 \pm 26.04
PTZ	917.8 (Stahl, 1997)	Weak	122 \pm 39.03	147 \pm 102.81
TDF	91.5 (Unger et al., 1982)	Moderate	31.8 \pm 2.48	160.5 \pm 281.71
FEN	88.5 (Hoffman et al., 1980)	Moderate	77.5 \pm 43.66	93.45 \pm 65.59
PRO	386.7 (Giknis, 1987)	Weak	78.6 \pm 28.92	141 \pm 17.47
TEB	275.8 (Becker et al., 1988)	Moderate	57.8 \pm 59.26	123 \pm 78.77
B595	–	Weak	36.7 \pm 14.24	33.7 \pm 10.84
B599	–	Potent	7.22 \pm 2.23	17.95 \pm 10.20
B600	–	Moderate	31.8 \pm 2.48	15.7 \pm 9.21

WEC vs EST MCZ is not included

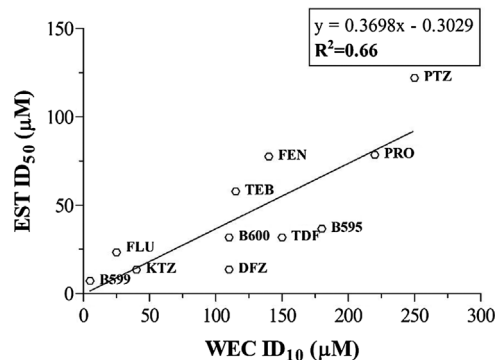
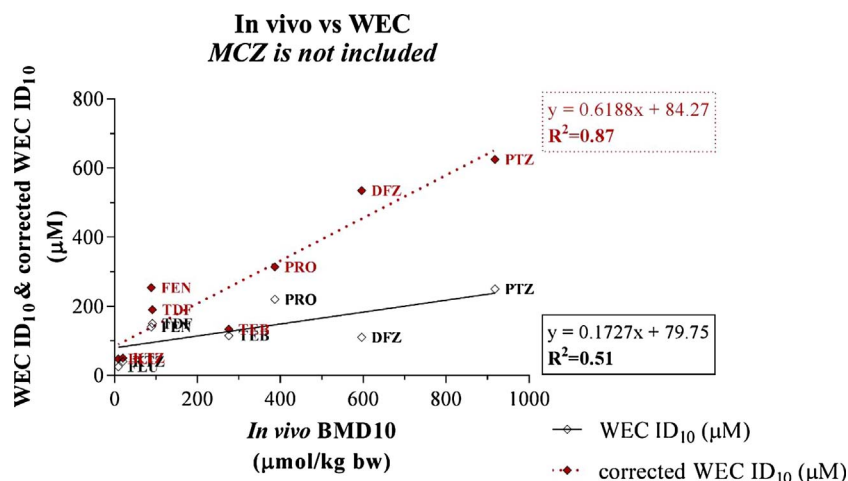


Fig. 4. Correlation between the ID values of eleven azoles tested in the WEC and EST.

external and internal signals in a more comprehensive manner (Fang et al., 2010; Robinson et al., 2012b; Robinson et al., 2010), compared to stem cells, which is a less complex multicellular system (Spielmann et al., 1997) and, therefore, their responses to any stimuli are likely more specific and probably restricted. For example, while examining the embryotoxic effects in rat WEC exposed to a chemical, we assessed a large number of morphological endpoints, including growth and differentiation parameters. On the other hand, the chemical assessment in the EST is based on microscopical observation of contracting cardiomyocytes only, which led to qualitative conclusions that could be less detailed compared to WEC (Piersma, 2006). Moreover, the limited applicability domain of EST (Augustine-Rauch et al., 2010; Piersma, 2006) and the limitations on the time window of each of the *in vitro* tests, may explain the differences in *in vitro* potency ranking of azoles between the WEC and EST, as well as their deviation from their *in vivo* embryotoxic potency (Piersma et al., 2014; Sogorb et al., 2014).

The co-implementation of the BeWo model, for correcting the ID₁₀ and ID₅₀ concentrations in WEC and EST led to considerable improvements in the predictability of both *in vitro* models of *in vivo* developmental toxicity, showing R^2 of 0.87 and 0.60, respectively. Previous studies showed that the BeWo model is quite well associated with the *ex vivo* placental model and, subsequently, it is an adequate model for initial screening the placental transfer rates of chemicals (Li et al., 2013; Poulsen et al., 2009; Prouillac and Lecoœur, 2010). The BeWo layer is a reductionistic model of the intact placenta, but it shows the importance of combining *in vitro* assays for designing batteries of alternative testing approaches (Bode et al., 2006; Mitra and Audus, 2008). The estimated relative Papp values showed that, although azoles belong to the same chemical group, their placental transfer rates diverge. In experiments in which the integrity of the BeWo layer was



shown to be intact, increased relative Papp values characterized increased transport of the chemical. However, attention should be given to those compounds that showed a low Papp value, such as B595, because they may have accumulated into the BeWo cells and, therefore, lead to false negative conclusions (Li et al., 2016). The elevated intracellular accumulation of B595 could be also linked to increased placental toxicity, which may be related to the increased *in vivo* post-implantation losses (Li et al., 2016). Furthermore, in this study, we showed that MCZ did not pass through the BeWo layer to the basolateral compartment (Fig. 3), but also even directly after its addition to the apical compartment it could not be detected (low recovery rate). MCZ might be bound to the polycarbonate membrane of the transwell plate or accumulated in the BeWo cells. Another explanation could be the metabolism of the parent compound, to MCZ-metabolites. Similarly to the human placenta, the BeWo cell layer has enzymatic activity, reflected by the expression of Cyp enzymes, *Cyp1a1*, *Cyp3a4* and *Cyp2c9* (Myllynen and Vähäkangas, 2013). The last two enzymes are also responsible for drug metabolism in the liver (Dvorak, 2011). Despite the fact that metabolism is a realistic aspect in *in vivo* and *in vitro* (when is applied) systems, the assumption of metabolism of MCZ in the BeWo cells might be unlikely because of short duration between exposure and sampling. Because of the poor ability of BeWo model to predict the placental transport rate of MCZ, we excluded MCZ from further analyses.

Here, we also observed that the estimated relative placental transfer rates were dependent on the molecular weight of the tested azoles, showing a very good correlation characterized with an R^2 of 0.70 (data not shown). KTZ was excluded from this association, because while it

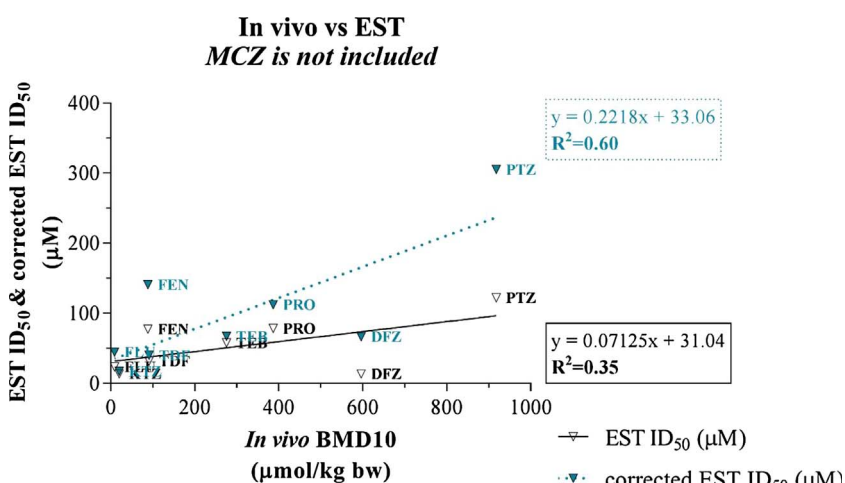


Fig. 5. Correlation of the *in vivo* BMD₁₀ (μmol/kg bw) with ID₁₀ (μM, ◇) and ID₁₀ as corrected with relative Papp values (μM, ◆), determined in the BeWo model, for eight azoles tested in the WEC, excluding MCZ and the three coded azoles obtained from BASF SE.

has the highest molecular weight (531.43 g/mol) of the selected tested azoles, its relative transport rate was estimated to 0.79, which was among the highest calculated values. In general, chemicals with low molecular weight are expected to pass easier through the *in vivo* placental barrier, while increased lipophilicity may additionally support their transport (Poulsen et al., 2009; Sastry, 1999). Similarly to the *in vivo* placental transfer, the transport of xenobiotics in the human *ex vivo* perfusion placental system is dependent on physicochemical properties (Poulsen et al., 2009), which may also affect the transport of chemicals through the BeWo cells due to high agreement between these two systems (Mitra and Audus, 2008). Therefore, supplementary research on the physicochemical and molecular properties of the tested compounds could further elucidate the mechanism of BeWo model transfer and explain the observed behaviour of both MCZ and KTZ in the present study. Furthermore, the characterization of possible interactions between the compounds and membrane transporters could give additional information for the permeability of chemicals through the BeWo layer (Li et al., 2015).

The RA concentration in mammals is regulated by *Dhrs3* and *Cyp26a1* expression, by synthesizing or metabolizing it, respectively, to maintain its balance for optimal embryonic growth and differentiation (Dimopoulou et al., 2016; Metzler and Sandell, 2016; Piersma et al., 2017; Tonk et al., 2015). Therefore, regulation of RA-related gene expression may be linked to embryotoxic responses (Luijten et al., 2010; Robinson et al., 2012b). In line with the functionality of these genes, in EST the strong embryotoxicants *in vitro*; FLU, MCZ and B599, upregulated *Dhrs3*. and downregulated *Cyp26a1*. In WEC, both these genes were upregulated. The rat WEC does have a more complex biological

Fig. 6. Correlation of the *in vivo* BMD₁₀ (μmol/kg bw) with ID₅₀ (μM, ▽) and ID₅₀ as corrected with relative Papp values (μM, ▽), determined in the BeWo model, for eight azoles tested in the EST, excluding MCZ and the three coded azoles obtained from BASF SE.

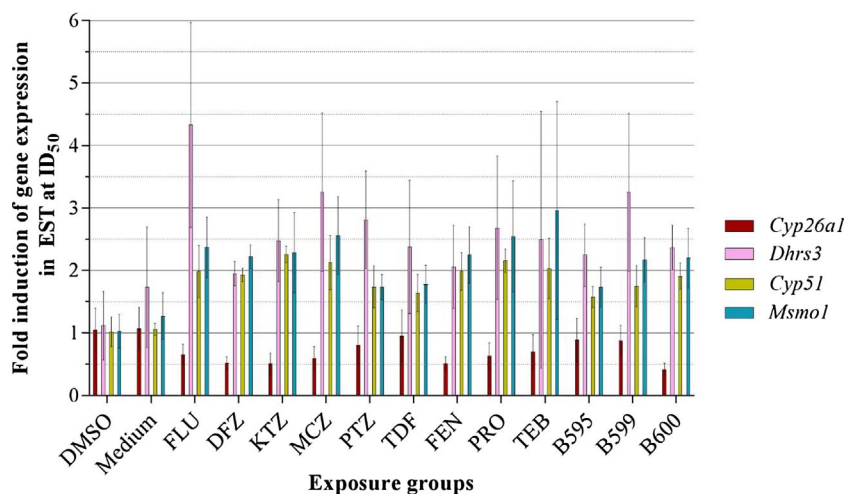


Fig. 7. Fold induction of four genes, Cyp26a1, Dhrs3, Cyp51 and Msmo1 in the EST exposed to ID₅₀ concentrations of each of the twelve azoles. Each bar represents a mean \pm SD (N = 8 for tested compounds and N = 12 for solvent control and medium control).

structure, organized as a whole network of more sophisticated responses, similar to *in vivo* embryos (Fang et al., 2010; Robinson et al., 2012b). Developmental effects are often localized to specific parts of embryos. Similarly, as illustrated in our previous study (Dimopoulou et al., 2016), the expression of Cyp26a1 is relatively high in the brain region and in the tail end of the embryo. Subsequently, by homogenization for quantifying gene expression changes in whole embryos, the dilution of the observed effects is inevitable, which may mask region-specific effects in the embryo. Therefore, EST may be a more straightforward *in vitro* screening system for detecting explicit RA related effects on the gene regulation level, due to its biological simplicity.

An additional factor that may determine the nature and magnitude of the effect of azoles on the expression of RA related genes in both *in vitro* systems (WEC and EST) is the chosen time window of exposure. Previous studies on the quantification of the gene expression effects on the level of EST transcriptome have suggested that differentiation in EST starts after plating aggregates on day 3 (van Dartel et al., 2010; van Dartel et al., 2011). In our previous studies (Dimopoulou et al., 2017a; Dimopoulou et al., 2016), we have shown that the early regulation of genes related to the differentiation process in the rat WEC could predict and precede the developmental toxic effects. Therefore, the transcriptional responses of the selected *in vitro* systems demonstrate a time-dependent fingerprinting, reflecting the dynamics of the embryonic differentiation, while revealing an increased predictivity in early gene responses governing the developmental process (Robinson et al., 2012c; Romero et al., 2015; van Dartel et al., 2010; van Dartel et al., 2011).

In the present research, we studied the expression of genes related to the fungicidal mode of action of the tested compounds in mammalian systems. The binding affinity of azoles to related mammalian enzymes is 100 times lower than in fungal systems. Consequently, the fungicidal mode of action is unlikely to play a role in the developmental toxicity of azoles (Trzaskos and Henry, 1989). Here, we observed that the effects on the regulation of the selected sterol-related genes in the EST followed the same pattern of expression as in the rat WEC. However, as in a previous study (Robinson et al., 2012c), the level of induction was greater in the case of gene expression studies in the EST, which may indicate differences in sensitivity between the systems and, subsequently, to the quick gene-mediated responses to chemical exposure. Both the selected genes (Cyp51 and Msmo1) are participating in the same step in the mammalian sterol biosynthesis pathway (Marotta and Tiboni, 2010; Santori et al., 2015). However, the higher induction of Msmo1 in screening sterol-mediated responses in both WEC and EST, supports our previous suggestion of replacing Cyp51 by Msmo1 for further compound testing as a major sterol-related biomarker for assessing relevant effects of chemicals in *in vitro* systems (Dimopoulou

et al., 2017b).

In conclusion, Dhrs3 and Msmo1 could be sensitive biomarkers for screening RA- and sterol-mediated responses, respectively, in both WEC and EST. Supportive results were observed in transcriptomics studies in the rat WEC, ZET and EST after exposure to azoles, in which the sensitivity of these genes suggested that they could be valuable candidate-biomarkers for revealing the mode of embryotoxicity and fungicidal activity of azoles, respectively (de Jong et al., 2011; Hermesen et al., 2012; Robinson et al., 2012c; van Dartel et al., 2011). The different gene regulatory patterns observed with different azoles point towards complex structure-activity relationships, which are difficult to elucidate based on the high structural complexity of the group of azoles.

In summary, we observed that the potency ranking of the *in vitro* developmental toxicity of the chemical class of azoles in the WEC and EST correlated quite well. Additionally, we showed that the *in vitro* prediction of *in vivo* developmental toxicity of azoles was notably improved when both WEC and EST were combined with the BeWo model, incorporating simple *in vitro* placental kinetics. Studying the differentially expressed genes in the EST exposed to the tested azoles, we revealed that Dhrs3 and Msmo1 were expressed within a similar pattern compared to their expression in the rat WEC. Considering the relatively high response magnitude of Dhrs3, as well as the detection of Cyp26a1 suppression in the EST, we suggested that EST might be an adequate *in vitro* system to screen direct RA-mediated effects on the level of the genome after exposure to azoles. However, answering intricate questions regarding the complexity of toxicological responses in more complex biological systems, WEC may be more informative. Overall, defining universal gene-biomarkers among the available *in vitro* systems may facilitate a better cross-model comparison and improve the *in vitro* – *in vivo* extrapolations for better predicting developmental toxicants.

Funding information

This work was supported by a collaborative project between Wageningen University (grant number 6153511466), RIVM and BASF SE.

Acknowledgements

We thank Conny van Oostrom and Hennie Hodemaekers for their technical support.

References

- Adeleye, Y., Andersen, M., Clewell, R., Davies, M., Dent, M., Edwards, S., Fowler, P., Malcomber, S., Nicol, B., Scott, A., Scott, S., Sun, B., Westmoreland, C., White, A., Zhang, Q., Carmichael, P.L., 2015. Implementing toxicity testing in the 21st century

- (TT21C): making safety decisions using toxicity pathways, and progress in a prototype risk assessment. *Toxicology* 332, 102–111.
- Adler, S., Basketter, D., Creton, S., Pelkonen, O., van Benthem, J., Zuang, V., Andersen, K.E., Angers-Loustau, A., Aptula, A., Bal-Price, A., Benfenati, E., Bernauer, U., Bessems, J., Bois, F.Y., Boobis, A., Brandon, E., Bremer, S., Broschard, T., Casati, S., Coecke, S., Corvi, R., Cronin, M., Daston, G., Dekant, W., Felter, S., Grignard, E., Gundert-Remy, U., Heinonen, T., Kimber, I., Kleinjans, J., Komulainen, H., Kreiling, R., Kreysa, J., Leite, S.B., Loizou, G., Maxwell, G., Mazzatorta, P., Munn, S., Pfuhler, S., Phrakonkham, P., Piersma, A., Poth, A., Prieto, P., Repetto, G., Rogiers, V., Schoeters, G., Schwarz, M., Serafimova, R., Tahti, H., Testai, E., van Delft, J., van Loveren, H., Vinken, M., Worth, A., Zaldivar, J.M., 2011. Alternative (non-animal) methods for cosmetics testing: current status and future prospects-2010. *Arch. Toxicol.* 85, 367–485.
- Augustine-Rauch, K., Zhang, C.X., Panzica-Kelly, J.M., 2010. In vitro developmental toxicology assays: a review of the state of the science of rodent and zebrafish whole embryo culture and embryonic stem cell assays. *Birth Defects Res. Part C Embryo Today: Rev.* 90, 87–98.
- Becker, H., Vogel, W., Terrier, C., 1988. Embryotoxicity study (including teratogenicity) with HWG 1608 technical in rat. Unpublished Report Ref No R 4451. Prepared by Research & Consulting Co AG (RCC), Itingen, Switzerland Submitted to WHO by Bayern AG, Leverkusen, Germany.
- Benirschke, K., Kaufmann, P., Baergen, R., 2006. *Pathology of the Human Placenta*. Springer, New York.
- Blaauboer, B.J., 2010. Biokinetic modeling and in vitro-in vivo extrapolations. *J. Toxicol. Environ. Health Part B Crit. Rev.* 13, 242–252.
- Bode, C.J., Jin, H., Rytting, E., Silverstein, P.S., Young, A.M., Audus, K.L., 2006. In vitro models for studying trophoblast transcellular transport. *Methods Mol. Med.* 122, 225–239.
- Brown, N.A., Fabro, S., 1981. Quantitation of rat embryonic development in vitro: a morphological scoring system. *Teratology* 24, 65–78.
- Daston, G.P., Naciff, J.M., 2010. Predicting developmental toxicity through toxicogenomics. *Birth Defects Res. Part C Embryo Today: Rev.* 90, 110–117.
- de Jong, E., Barenys, M., Hermsen, S.A., Verhoef, A., Ossendorp, B.C., Bessems, J.G., Piersma, A.H., 2011. Comparison of the mouse Embryonic Stem cell Test, the rat Whole Embryo Culture and the Zebrafish Embryotoxicity Test as alternative methods for developmental toxicity testing of six 1,2,4-triazoles. *Toxicol. Appl. Pharmacol.* 253, 103–111.
- Dimopoulou, M., Verhoef, A., van Ravenzwaay, B., Rietjens, I.M., Piersma, A.H., 2016. Flusilazole induces spatio-temporal expression patterns of retinoic acid-, differentiation- and sterol biosynthesis-related genes in the rat Whole Embryo Culture. *Reprod. Toxicol. (Elmsford, NY)* 64, 77–85.
- Dimopoulou, M., Verhoef, A., Pennings, J.L.A., van Ravenzwaay, B., Rietjens, I., Piersma, A.H., 2017a. Embryotoxic and pharmacologic potency ranking of six azoles in the rat whole embryo culture by morphological and transcriptomic analysis. *Toxicol. Appl. Pharmacol.* 322, 15–26.
- Dimopoulou, M., Verhoef, A., Pennings, J.L.A., van Ravenzwaay, B., Rietjens, I.M.C.M., Piersma, A.H., 2017b. A transcriptomic approach for evaluating the relative potency and mechanism of action of azoles in the rat Whole Embryo Culture. *Toxicology* 392, 96–105.
- Doetschman, T.C., Eistetter, H., Katz, M., Schmidt, W., Kemler, R., 1985. The in vitro development of blastocyst-derived embryonic stem cell lines: formation of visceral yolk sac, blood islands and myocardium. *J. Embryol. Exp. Morphol.* 87, 27–45.
- Dvorak, Z., 2011. Drug-drug interactions by azole antifungals: beyond a dogma of CYP3A4 enzyme activity inhibition. *Toxicol. Lett.* 202, 129–132.
- Ellis-Hutchings, R.G., Carney, E.W., 2010. Whole embryo culture: a new technique that enabled decades of mechanistic discoveries. *Birth Defects Res. Part B: Dev. Reprod. Toxicol.* 89, 304–312.
- Estevan, C., Fuster, E., del Río, E., Pamiés, D., Vilanova, E., Sogorb, M.A., 2014. Organophosphorus pesticide chlorpyrifos and its metabolites alter the expression of biomarker genes of differentiation in D3 mouse embryonic stem cells in a comparable way to other model neurodevelopmental toxicants. *Chem. Res. Toxicol.* 27, 1487–1495.
- Fang, H., Yang, Y., Li, C., Fu, S., Yang, Z., Jin, G., Wang, K., Zhang, J., Jin, Y., 2010. Transcriptome analysis of early organogenesis in human embryos. *Dev. Cell* 19, 174–184.
- Genschow, E., Spielmann, H., Scholz, G., Pohl, I., Seiler, A., Clemann, N., Bremer, S., Becker, K., 2004. Validation of the embryonic stem cell test in the international ECVAM validation study on three in vitro embryotoxicity tests. *Altern. Lab. Anim.: ATLA* 32, 209–244.
- Georgopapadakou, N.H., 1998. Antifungals: mechanism of action and resistance, established and novel drugs. *Curr. Opin. Microbiol.* 1, 547–557.
- Giknis, M.L.A., 1987. A teratology (segment II) study in rats. Unpublished Report No: 86004 from Ciba-Geigy Pharmaceutical Division. New Jersey Submitted to WHO by Ciba-Geigy Ltd, Basle, Switzerland.
- Hermes, S.A., Pronk, T.E., van den Brandhof, E.J., van der Ven, L.T., Piersma, A.H., 2012. Triazole-induced gene expression changes in the zebrafish embryo. *Reprod. Toxicol. (Elmsford, NY)* 34, 216–224.
- Hoffman, D.G., Owen, N.V., Adams, E.R., 1980. A teratology study with EL-222 in the rat. Unpublished Report No R06279 Form Lilly Research Laboratories, USA. Submitted to WHO by DowElanco Europe, Wantage, Oxon, United Kingdom.
- Ito, C., Shibutani, Y., Inoue, K., Nakano, K., Ohnishi, H., 1976. Toxicological studies of miconazole (II) teratological studies of miconazole in rats. *Iyakuken Kenkyu* 7, 367–376.
- Krewski, D., Acosta Jr., D., Andersen, M., Anderson, H., Bailar 3rd, J.C., Boekelheide, K., Brent, R., Charney, G., Cheung, V.G., Green Jr., S., Kelsey, K.T., Kerkvliet, N.I., Li, A.A., McCray, L., Meyer, O., Patterson, R.D., Pennie, W., Scala, R.A., Solomon, G.M., Stephens, M., Yager, J., Zeise, L., 2010. Toxicity testing in the 21st century: a vision and a strategy. *J. Toxicol. Environ. Health B Crit. Rev.* 13, 51–138.
- Lamontia, C.L., Staples, R.E., Alvarez, L., 1984. Embryo-fetal toxicity and teratogenicity study of INH-6573-39 by gavage in the rat. Unpublished Reports No HLR 444-83 and HLR 142-84 from Haskell Laboratory for Toxicology and Industrial Medicine, Wilmington, Delaware, USA. Submitted to WHO by El du Pont de Nemours & Co, Inc, Wilmington, Delaware, USA. Summarized in *JMPR Monograph—Flusilazole, Pesticide residues in food: 1995 evaluations Part II Toxicological & Environment*. <http://www.inchem.org/documents/jmpr/jmpmono/v95pr08.htm>.
- Lee, H.Y., Inselman, A.L., Kanungo, J., Hansen, D.K., 2012. Alternative models in developmental toxicology. *Syst. Biol. Reprod. Med.* 58, 10–22.
- Li, H., van Ravenzwaay, B., Rietjens, I.M., Louise, J., 2013. Assessment of an in vitro transport model using BeWo b30 cells to predict placental transfer of compounds. *Arch. Toxicol.* 87, 1661–1669.
- Li, H., Rietjens, I.M.C.M., Louise, J., Blok, M., Wang, X., Snijders, L., van Ravenzwaay, B., 2015. Use of the ES-D3 cell differentiation assay, combined with the BeWo transport model, to predict relative in vivo developmental toxicity of antifungal compounds. *Toxicol. In Vitro* 29, 320–328.
- Li, H., Flick, B., Rietjens, I.M.C.M., Louise, J., Schneider, S., van Ravenzwaay, B., 2016. Extended evaluation on the ES-D3 cell differentiation assay combined with the BeWo transport model, to predict relative developmental toxicity of triazole compounds. *Arch. Toxicol.* 90, 1225–1237.
- Lochry, E.A., 1987. Developmental toxicity study of CGA-169374 technical (FL-851406) administered orally via gavage to Crl:COBS CD (SD) BR presumed pregnant rats. Unpublished Report No 203-005 From Novartis Crop Protection AG, Basel, Switzerland and Argus Research Lab Inc, Horsham, USA. Submitted to WHO by Syngenta Crop Protection AG, Basel, Switzerland http://apps.who.int/iris/bitstream/10665/44064/1/9789241665230_engpdf?ua=1.
- Luijten, M., van Beelen, V.A., Verhoef, A., Renkens, M.F., van Herwijnen, M.H., Westerman, A., van Schooten, F.J., Pennings, J.L., Piersma, A.H., 2010. Transcriptomics analysis of retinoic acid embryotoxicity in rat postimplantation whole embryo culture. *Reprod. Toxicol. (Elmsford, NY)* 30, 333–340.
- Marotta, F., Tiboni, G.M., 2010. Molecular aspects of azoles-induced teratogenesis. *Expert Opin. Drug Metab. Toxicol.* 6, 461–482.
- Marx-Stoelting, P., Adriaens, E., Ahr, H.J., Bremer, S., Garthoff, B., Gelbke, H.P., Piersma, A., Pellizzer, C., Reuter, U., Rogiers, V., Schenk, B., Schwengberg, S., Seiler, A., Spielmann, H., Steemans, M., Stedman, D.B., Vanparys, P., Vericat, J.A., Verwei, M., van der Water, F., Weimer, M., Schwarz, M., 2009. A review of the implementation of the embryonic stem cell test (EST): the report and recommendations of an ECVAM/ReProTect Workshop. *Altern. Lab. Anim.: ATLA* 37, 313–328.
- Metzler, M.A., Sandell, L.L., 2016. Enzymatic metabolism of vitamin A in developing vertebrate embryos. *Nutrients* 8, 812.
- Mitra, P., Audus, K.L., 2008. In vitro models and multidrug resistance mechanisms of the placental barrier. In: Ehrhardt, C., Kim, K.-J. (Eds.), *Drug Absorption Studies: In Situ, In Vitro and In Silico Models*. Springer, US, Boston, MA, pp. 368–396.
- Myllynen, P., Vähäkangas, K., 2013. Placental transfer and metabolism: an overview of the experimental models utilizing human placental tissue. *Toxicol. In Vitro* 27, 507–512.
- Myllynen, P., Pasanen, M., Pelkonen, O., 2005. Human placenta: a human organ for developmental toxicology research and biomonitoring. *Placenta* 26, 361–371.
- New, D.A.T., 1978. Whole-embryo culture and the study of mammalian embryos during organogenesis. *Biol. Rev.* 53, 81–122.
- Pacifici, G.M., Nottoli, R., 1995. Placental transfer of drugs administered to the mother. *Clin. Pharmacokinet.* 28, 235–269.
- Piersma, A.H., Genschow, E., Verhoef, A., Spanjersberg, M.Q., Brown, N.A., Brady, M., Burns, A., Clemann, N., Seiler, A., Spielmann, H., 2004. Validation of the post-implantation rat whole-embryo culture test in the international ECVAM validation study on three in vitro embryotoxicity tests. *Altern. Lab. Anim.: ATLA* 32, 275–307.
- Piersma, A.H., Bosgra, S., van Duursen, M.B., Hermsen, S.A., Jonker, L.R., Kroese, E.D., van der Linden, S.C., Man, H., Roelofs, M.J., Schulpen, S.H., Schwarz, M., Uibel, F., van Vugt-Lussenburg, B.M., Westerhout, J., Wolterbeek, A.P., van der Burg, B., 2013. Evaluation of an alternative in vitro test battery for detecting reproductive toxicants. *Reprod. Toxicol. (Elmsford, NY)* 38, 53–64.
- Piersma, A.H., Ezendam, J., Luijten, M., Muller, J.J., Rorije, E., van der Ven, L.T., van Benthem, J., 2014. A critical appraisal of the process of regulatory implementation of novel in vivo and in vitro methods for chemical hazard and risk assessment. *Crit. Rev. Toxicol.* 44, 876–894.
- Piersma, A.H., Hessel, E.V., Staal, Y.C., 2017. Retinoic acid in developmental toxicology: teratogen, morphogen and biomarker. *Reprod. Toxicol. (Elmsford, NY)* 72, 53–61.
- Piersma, A.H., 2006. Alternative methods for developmental toxicity testing. *Basic Clin. Pharmacol. Toxicol.* 98, 427–431.
- Poulsen, M.S., Rytting, E., Mose, T., Knudsen, L.E., 2009. Modeling placental transport: correlation of in vitro BeWo cell permeability and ex vivo human placental perfusion. *Toxicol. In Vitro* 23, 1380–1386.
- Prouillac, C., Lecoq, S., 2010. The role of the placenta in fetal exposure to xenobiotics: importance of membrane transporters and human models for transfer studies. *Drug Metab. Dispos.: Biol. Fate Chem.* 38, 1623–1635.
- Robinson, J.F., Piersma, A.H., 2013. Toxicogenomic approaches in developmental toxicology testing. *Methods Mol. Biol. (Clifton, NJ)* 947, 451–473.
- Robinson, J.F., van Beelen, V.A., Verhoef, A., Renkens, M.F., Luijten, M., van Herwijnen, M.H., Westerman, A., Pennings, J.L., Piersma, A.H., 2010. Embryotoxicant-specific transcriptomic responses in rat postimplantation whole-embryo culture. *Toxicol. Sci.: Off. J. Soc. Toxicol.* 118, 675–685.
- Robinson, J.F., Pennings, J.L., Piersma, A.H., 2012a. A review of toxicogenomic approaches in developmental toxicology. *Methods Mol. Biol. (Clifton, NJ)* 889, 347–371.

- Robinson, J.F., Tonk, E.C.M., Verhoef, A., Piersma, A.H., 2012b. Triazole induced concentration-related gene signatures in rat whole embryo culture. *Reprod. Toxicol.* 34, 275–283.
- Robinson, J.F., Verhoef, A., Pennings, J.L., Pronk, T.E., Piersma, A.H., 2012c. A comparison of gene expression responses in rat whole embryo culture and in vivo: time-dependent retinoic acid-induced teratogenic response. *Toxicol. Sci.: Off. J. Soc. Toxicol.* 126, 242–254.
- Romero, A.C., del Río, E., Vilanova, E., Sogorb, M.A., 2015. RNA transcripts for the quantification of differentiation allow marked improvements in the performance of embryonic stem cell test (EST). *Toxicol. Lett.* 238, 60–69.
- Rovida, C., Hartung, T., 2009. Re-evaluation of animal numbers and costs for in vivo tests to accomplish REACH legislation requirements for chemicals – a report by the transatlantic think tank for toxicology (t(4)). *Altex* 26, 187–208.
- Santori, F.R., Huang, P., van de Pavert, S.A., Douglass Jr., E.F., Leaver, D.J., Haubrich, B.A., Keber, R., Lorbek, G., Konijn, T., Rosales, B.N., Rozman, D., Horvat, S., Rahier, A., Mebius, R.E., Rastinejad, F., Nes, W.D., Littman, D.R., 2015. Identification of natural RORgamma ligands that regulate the development of lymphoid cells. *Cell Metab.* 21, 286–297.
- Sastry, B.V.R., 1999. Techniques to study human placental transport. *Adv. Drug Deliv. Rev.* 38, 17–39.
- Scialli, A.R., Guikema, A.J., 2012. REACH and reproductive and developmental toxicology: still questions. *Syst. Biol. Reprod. Med.* 58, 63–69.
- Scialli, A.R., 2008. The challenge of reproductive and developmental toxicology under REACH. *Regul. Toxicol. Pharmacol.: RTP* 51, 244–250.
- Slob, W., 2002. Dose-response modeling of continuous endpoints. *Toxicol. Sci.* 66, 298–312.
- Sogorb, M.A., Pamies, D., de Lapuente, J., Estevan, C., Estevez, J., Vilanova, E., 2014. An integrated approach for detecting embryotoxicity and developmental toxicity of environmental contaminants using in vitro alternative methods. *Toxicol. Lett.* 230, 356–367.
- Spielmann, H., Pohl, I., Doering, B., Liebsch, M., Moldenhauer, F., 1997. The embryonic stem cell test (EST), an in vitro embryotoxicity test using two permanent mouse cell lines: 3T3 fibroblasts and embryonic stem cells. *In Vitro Toxicol.* 10, 119–127.
- Spielmann, H., 2009. The way forward in reproductive/developmental toxicity testing. *Altern. Lab. Anim.: ATLA* 37, 641–656.
- Stahl, B., 1997. JAU 6476 – Developmental toxicity study in rats after oral administration. Unpublished Report No. M-012279-01-1 from Bayer AG, Wuppertal, Germany. Submitted to WHO by Bayer CropScience AG, Germany. https://www.google.nl/url?sa=t&rct=j&q=&esrc=s&source=web&cd=2&ved=0ahUKEwjNcX5-HPAhWDrxokHebSDzYQFgghMAE&url=http%3A%2F%2Fapps.who.int%2Fpesticide-residues-jmpr-database%2Fdocument%2F110&usg=AFQjCNGpjQOE2xfb0QbWPWwA5-avbrC8kQ&sig2=ZFM7G3fgK4EdIA0e_zX0hQ&cad=rja.
- Strikwold, M., Spenkelink, B., Woutersen, R.A., Rietjens, I.M., Punt, A., 2013. Combining in vitro embryotoxicity data with physiologically based kinetic (PBK) modelling to define in vivo dose-response curves for developmental toxicity of phenol in rat and human. *Arch. Toxicol.* 87, 1709–1723.
- Tachibana, M., Noguchi, Y., Monro, A.M., 1987. Toxicology of fluconazole in experimental animals. In: Fromtling, R.A. (Ed.), *Recent Trends in the Discovery, Development, and Evaluation of Antifungal Agents*. JR Prous, Barcelona, pp. 93–102.
- Tonk, E.C., Pennings, J.L., Piersma, A.H., 2015. An adverse outcome pathway framework for neural tube and axial defects mediated by modulation of retinoic acid homeostasis. *Reprod. Toxicol. (Elmsford, NY)* 55, 104–113.
- Trzaskos, J.M., Henry, M.J., 1989. Comparative effects of the azole-based fungicide flusilazole on yeast and mammalian lanosterol 14 alpha-methyl demethylase. *Antimicrob. Agents Chemother.* 33, 1228–1231.
- Unger, T.M., Van Goethem, D., Shellenberger, T.E., 1982. A teratological evaluation of Bayleton in mated female rats. Report No 324 to Mobay Chemical Corporation Agricultural Chemical Division Submitted to WHO by Bayer AG (Unpublished). Midwest Research Institute. <http://www.winchem.org/documents/jmpr/jmpmono/v83pr39htm>.
- van Dartel, D.A., Pennings, J.L., van Schooten, F.J., Piersma, A.H., 2010. Transcriptomics-based identification of developmental toxicants through their interference with cardiomyocyte differentiation of embryonic stem cells. *Toxicol. Appl. Pharmacol.* 243, 420–428.
- van Dartel, D.A.M., Pennings, J.L.A., de la Fonteyne, L.J.J., Brauers, K.J.J., Claessen, S., van Delft, J.H., Kleinjans, J.C.S., Piersma, A.H., 2011. Concentration-dependent gene expression responses to flusilazole in embryonic stem cell differentiation cultures. *Toxicol. Appl. Pharmacol.* 251, 110–118.
- van der Jagt, K., Munn, S., Tørsløv, J., de Bruijn, J., 2004. *Alternative Approaches can Reduce the Use of Test Animals Under Reach* European Commission Directorate General JRC Joint Research Centre. Institute for Health and Consumer Protection. <http://home.kpn.nl/reach/downloads/reducingtheuseoftestanimalsunderreachihcpreporpdf>.
- Webster, W.S., Brown-Woodman, P.D., Ritchie, H.E., 1997. A review of the contribution of whole embryo culture to the determination of hazard and risk in teratogenicity testing. *Int. J. Dev. Biology* 41, 329–335.